J. Fluid Mech. (1978), *vol.* 88, *part* 3, *pp.* 563–583
Printed in Great Britain

The development and structure of turbulent plane jets

By K. W. EVERITT† AND A. G. ROBINS‡
Department of Aeronautics, Imperial College, London

(Received 15 August 1977 and in revised form 12 May 1978)

The structure and development of turbulent plane jets in still air and moving streams are described. The nature of the small-scale turbulence cannot be accurately ascertained because of the difficulties inherent in the measurement of dissipation in highly turbulent flows. Although correlation measurements in a jet in still air indicate a large-scale structure which can best be described as 'local flapping', measurements in a jet in a moving stream do not reveal a similar structure. The development of the turbulence structure in a jet in a moving parallel stream is described and the properties of turbulent jets and wakes are shown to be reasonably well predicted by the use of a variable-eddy-viscosity formula together with the formal self-preserving properties of the equations of motion.

1. Introduction

Although there are several published papers concerning the structure and development of two-dimensional jets in still air (Gutmark & Wygnanski 1976; Heskestad 1965*a*) and in parallel moving streams (Bradbury 1965; Bradbury & Riley 1967) a complete description of these flows cannot be said to exist. The purpose of the current publication is to present and discuss those results of experiments undertaken by the authors (Everitt 1972; Robins 1973) which either extend or modify the existing body of literature concerning plane turbulent jets. Significant differences are found to exist between the results of investigations undertaken with similar experimental techniques and, as a result, it is suggested that further work be carried out using pulsed hot-wire or laser anemometers.

Large experimental errors are implicit in the use of hot-wire anemometers in a jet in still air because of the high turbulent intensities in the outer regions of the flow. The existence of a parallel moving stream external to the jet greatly reduces these problems as the mean streamwise velocity in the outer part of the flow no longer tends to zero. However, the flow of a jet in a moving stream is similar to that of a jet in still air only when the excess velocity on the centre-line is large with respect to the free-stream velocity. In practice, a jet in a moving stream is an approximately self-preserving flow, whereas a jet in still air is an exactly self-preserving flow. An interesting feature of the former is that two states of self-preservation are possible, one when the excess centre-line velocity is much greater than the free-stream velocity and the other when the excess centre-line velocity is much smaller than the free-stream velocity.

† Present address: University of Warwick, Coventry CV4 7AL.
‡ Present address: Marchwood Engineering Laboratories, Hampshire SO4 4ZB.

The latter case is similar to a wake flow far downstream of a body. To differentiate between the two cases the terms 'strong jet' and 'weak jet' will be used; the former including a jet in still air. By analogy with wake flows, it is to be expected that the self-preserving weak jet will be slow to develop, so that most experiments on jets in moving streams will reveal a structure which is slowly developing over a substantial streamwise fetch.

2. Apparatus and instrumentation

The jet blowing equipment used by Robins (1973) consisted of a variable-speed centrifugal fan supplying air through a settling chamber and contraction to a nozzle unit. The jet issued from the nozzle via a slot of span $s = 16$ in. whose height h could be varied from $\frac{1}{8}$ to 1 in. in steps of $\frac{1}{8}$ in. The flow downstream of the nozzle was constrained between two parallel side walls, 16 in. apart, which extended upstream of the nozzle and, except at their downstream ends, were flared onto a semicircular lip. This apparatus was later used by Goldschmidt & Bradshaw (1973) in their investigation of possible jet 'flapping' motions. For the work on a jet issuing into a parallel moving stream (Everitt 1972) a nozzle unit was incorporated into the trailing edge of a two-dimensional wing of symmetrical cross-section which spanned the working section of the Imperial College 3×2 ft closed-return wind tunnel. The wing was supplied with air by a centrifugal fan situated beneath the tunnel; a set of 72 closely spaced corner vanes was used to turn the incoming flow from the fan through 90° into a 24 in. by 1 in. duct and thence, via a contraction, to the 24 in. by $\frac{3}{16}$ in. nozzle exit slot. It was found that away from the wall layers the flow from both nozzles was satisfactorily two-dimensional.

Measurements were made using Pitot tubes and linearized constant-temperature hot-wire anemometers with a single wire, a single inclined wire and crossed wires. In most respects the techniques were the same as those used by Gutmark & Wygnanski (1976). Hot-wire results were corrected for tangential cooling (Champagne, Sleicher & Wehrmann 1967); Guitton (1968) has suggested that this accounts for most of the experimental error in the determination of the normal stresses in the central region of the flow. No further corrections were applied and it is to be expected that the results in the outer regions of the jets issuing into still air are significantly in error because of the high ratio of the velocity fluctuations to the local mean velocity. It is unlikely that correction formulae can be applied in this area as many of the assumptions implicit in the development of hot-wire response equations are untenable. In this respect the data obtained from jets issuing into weak external streams give a better guide to the structure of the outer regions of the flow.

3. Flow development

For the jets issuing into still air the development of the centre-line mean velocity U_0 and longitudinal turbulence intensity $\overline{u^2}$ was investigated for a range of nozzle conditions, and the results obtained were used to estimate the length x_1 of the potential-core region and the position $x = x_2$ at which the flow became fully developed. The variation of x_1 and x_2 with the nozzle conditions is compared with the results of

Source	$U_j h/\nu$	h (in.)	s/h	x_1/h	x_2/h
Robins	16×10^3	0·125	128	6–7	70–100
	30×10^3	0·25	64	5–7	40–60
	30×10^3	0·50	32	5	20–35
	75×10^3	0·75	21	5	20–30
Heskestad	34×10^3	0·5	120	7	65†
Gutmark & Wygnanski	30×10^3	0·512	38	—	30–40
Bradbury	30×10^3	0·375	47	—	40–60
Everitt	25×10^3	0·1875	128	—	†

† True self-preservation not attained.

TABLE 1. Characteristic parameters of developing jet flows.

other studies in table 1 (in which U_j is the jet exit velocity and ν is the kinematic viscosity). As consideration of the spread of the shear layers downstream of the nozzle lip indicates, x_1/h is substantially constant. However, it is interesting to note, though difficult to explain, that x_2/h appears to be directly related to the nozzle aspect ratio s/h. It is not clear from the data whether x_2/h tends to a constant asymptotic value for large aspect ratios. Throughout the range of the Reynolds number $U_j h/\nu$, which varied from 7×10^3 to 75×10^3, no Reynolds number effects were evident, except possibly at the lowest value. Although the aspect ratio of the jets issuing into a parallel moving stream was not varied, the ratio U_j/U_1 of the jet exit velocity to the free-stream velocity was varied from 2·6 to 17. (For such a flow self-preservation is possible as long as the ratio of the excess velocity U_0 on the jet centre-line to the free-stream velocity is much greater than unity. Bradbury (1965) suggested that this ratio does not, in practice, need to be much greater than unity.) If at a given station the flow structure depends only on the excess momentum flux introduced by the jet then, at a given x/h, the non-dimensional longitudinal intensity $\overline{u^2}/U_0^2$ is a function of U_1/U_0 only. The present results (figure 1) indicate that for low ratios of the jet exit velocity to the free-stream velocity the precise nozzle conditions influence the flow for a considerable distance downstream; e.g. the influence extends to about $x = 160h$ if $U_j/U_1 < 3{\cdot}6$ and to about $230h$ if $U_j/U_1 < 2{\cdot}9$.

It is convenient to define the local jet thickness δ as the distance from the jet centre-line to the point where the excess velocity has fallen to one-half of its centre-line value. For jet flows, the rate of spread $d\delta/dx$ and mean-velocity decay rate

$$d(U_j/U_0)^2/d(x/h)$$

are generally in good agreement (table 2). However, the positions of the virtual origin are not obviously related to the nozzle conditions (see also Bradbury 1967). For a jet in a moving stream the hypothesis that the flow some way downstream of the nozzle is independent of the precise nozzle conditions leads to the result that the length scale to be used in considerations of the flow development is the momentum thickness θ of the jet, where

$$\theta = \int_{-\infty}^{\infty} \frac{U}{U_1}\left(\frac{U}{U_1} - 1\right) dy.$$

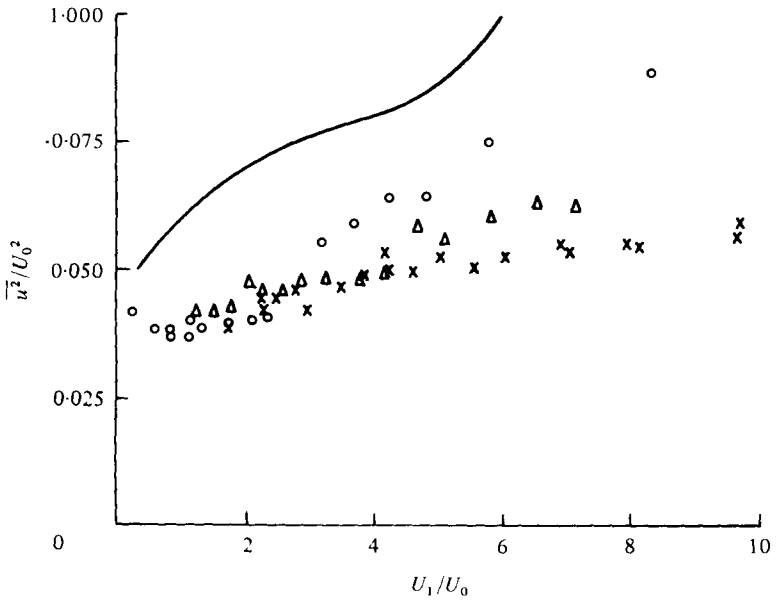

FIGURE 1. Variation of centre-line longitudinal turbulence with excess velocity ratio. x/h: ○, 163; △, 230; ×, 322; ——, 250, Bradbury & Riley.

Source	h (in.)	$\frac{d(\delta/h)}{d(x/h)}$	$\frac{d(U_j^2/U_0^2)}{d(x/h)}$	$\frac{\overline{u^2}}{U_0^2}$†	$\frac{\overline{v^2}}{U_0^2}$†	$\frac{\overline{w^2}}{U_0^2}$†	$\frac{q^2}{U_0^2}$§
Jet in still air							
Robins	0·125	0·10	0·18–0·21	0·053	—	—	—
	0·25	0·10–0·11	0·17–0·19	0·050	0·044	0·036	0·130
	0·50	0·11	0·14–0·18	0·049	—	—	—
	0·75	0·09	0·19–0·22	0·061	—	—	—
Heskestad	0·50	0·11	0·16	0·070‡	0·034	0·042	0·146
Gutmark & Wygnanski	0·512	0·10	0·17	0·074	0·043	0·035	0·152
Jet in moving stream							
Bradbury	0·375	0·11	0·16	0·044	0·057	0·034	0·155
Everitt	0·1875	—	0·18	0·038*	0·038*	0·024*	0·100*

† Centre-line values in fully developed flow.
‡ Rising to 0·108.
§ $\overline{q^2} = \overline{u^2}+\overline{v^2}+\overline{w^2}$.
* 'Strong' jet values.

TABLE 2. Characteristic parameters of developed jet flows.

The collapse of the data on the jet spread and the decay of the centre-line mean velocity presented in figures 2 and 3 supports the above hypothesis and the absence of any requirement to apply virtual-origin shifts suggests that the data represent an improvement on previously published results. It can be seen from table 2 that, although the results for the rate of spread and velocity decay for jets in still air and for strong jets ($U_0/U_1 > 5$) in a moving stream are reasonably consistent (for further dis-

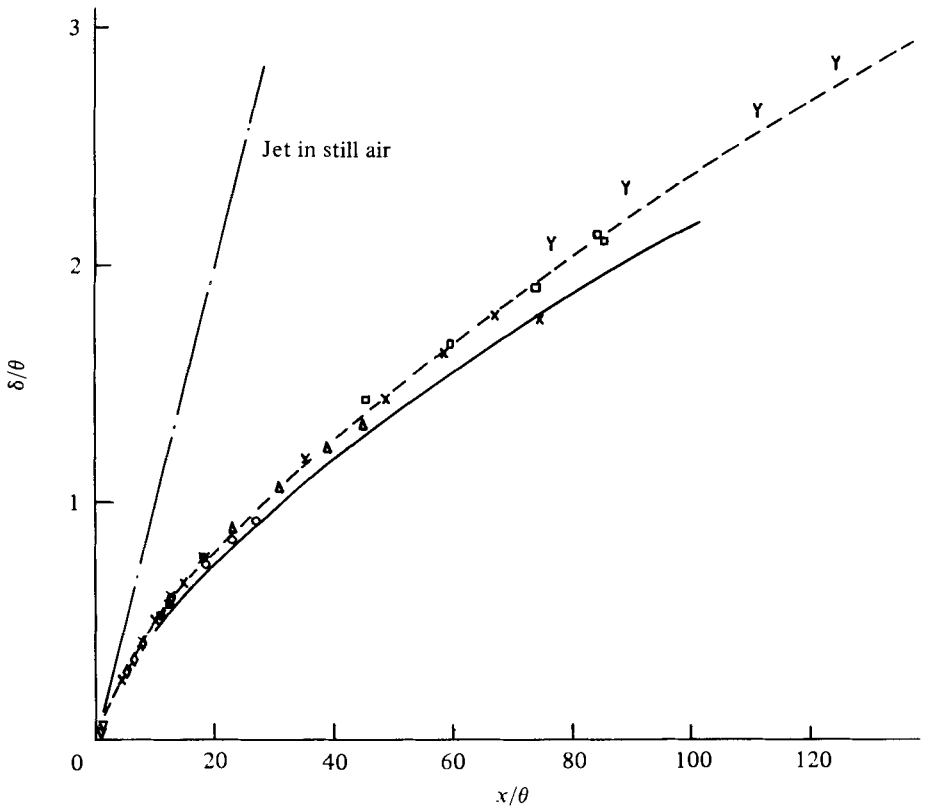

FIGURE 2. Variation of jet spread with downstream distance. U_j/U_1: ▽, 17·08; ◇, 6·72; ○, 4·48; △, 3·78; ×, 3·29; ⊙, 3·24; □, 3·03; Y, 2·60; +, 1·72, Bradbury.

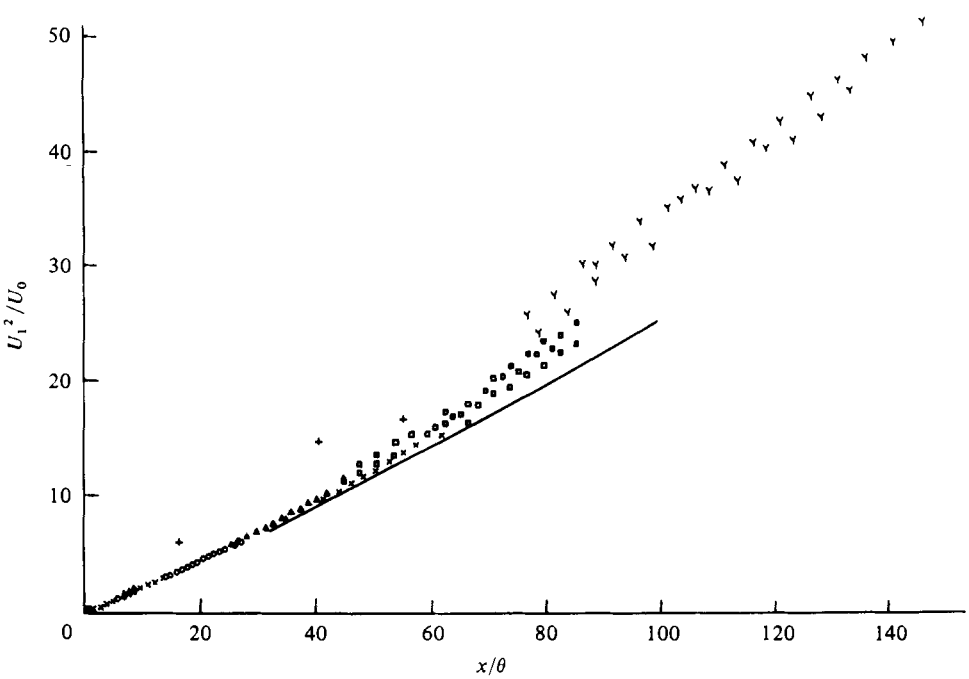

FIGURE 3. Centre-line mean velocity decay. Symbols as in figure 2.

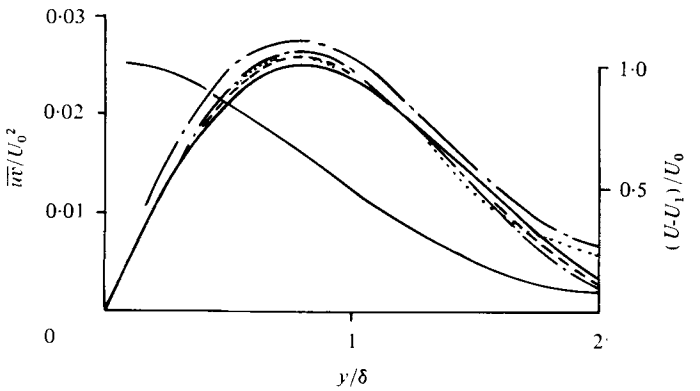

FIGURE 4. Mean-velocity and shear-stress profiles for strong jets. ——, Robins; – – – –, Everitt; ———, Heskestad; – – –, Bradbury; ·····, Gutmark & Wygnanski.

cussion of this point see Kotsovinos 1976; Bradshaw 1977), considerable scatter exists in the values of the centre-line turbulent intensities in the fully developed flows. It should be noted that Heskestad's results for $\overline{u^2}/U_0^2$ decrease as the Reynolds number increases from $4{\cdot}7 \times 10^3$ to 37×10^3 and must therefore be treated with some caution. A further point of interest is that, although Gutmark & Wygnanski's data show all three turbulence components developing at the same rate, the present results for jets in still air show that close to the nozzle $\overline{v^2}$ tends to develop most rapidly, whereas further downstream $\overline{u^2}$ develops most rapidly. However, the differences are nowhere large and all three components appear to reach their fully developed values at about the same position.

4. The strong jet

4.1. *Structure of the developed flow*

It has already been noted that the turbulence levels in the developed flow show considerable scatter from one investigation to another. Results obtained for $y/\delta > 1{\cdot}5$ on a jet in still air must be considered very unreliable as there is a significant probability of instantaneously reversed flow and yaw angles in excess of 45°; e.g. at $y = 1{\cdot}5\delta$, $P(U+u<0) \sim 0{\cdot}1$. Further, because of these high local intensities, it is very unlikely that agreement will exist between measured shear-stress profiles and those calculated from the momentum equation using measured mean-velocity and normal-stress data. Although Bradbury and Gutmark & Wygnanski report good agreement this is the result of neglecting the normal-stress terms in the momentum equation, which increase the maximum calculated shear stress by about 10 %. However, relatively good agreement exists between the various calculated values shown in figure 4, which were derived from

$$\frac{\partial \overline{uv}}{\partial y} = -U\frac{\partial U}{\partial x} - V\frac{\partial U}{\partial y} - \frac{\partial(\overline{u^2}-\overline{v^2})}{\partial x}.$$

Also shown in this figure is a typical mean-velocity profile which is in accord with other investigations. The normal-stress profiles show fairly large variations from one investigation to another (figure 5). At first sight the results lead one to suspect that

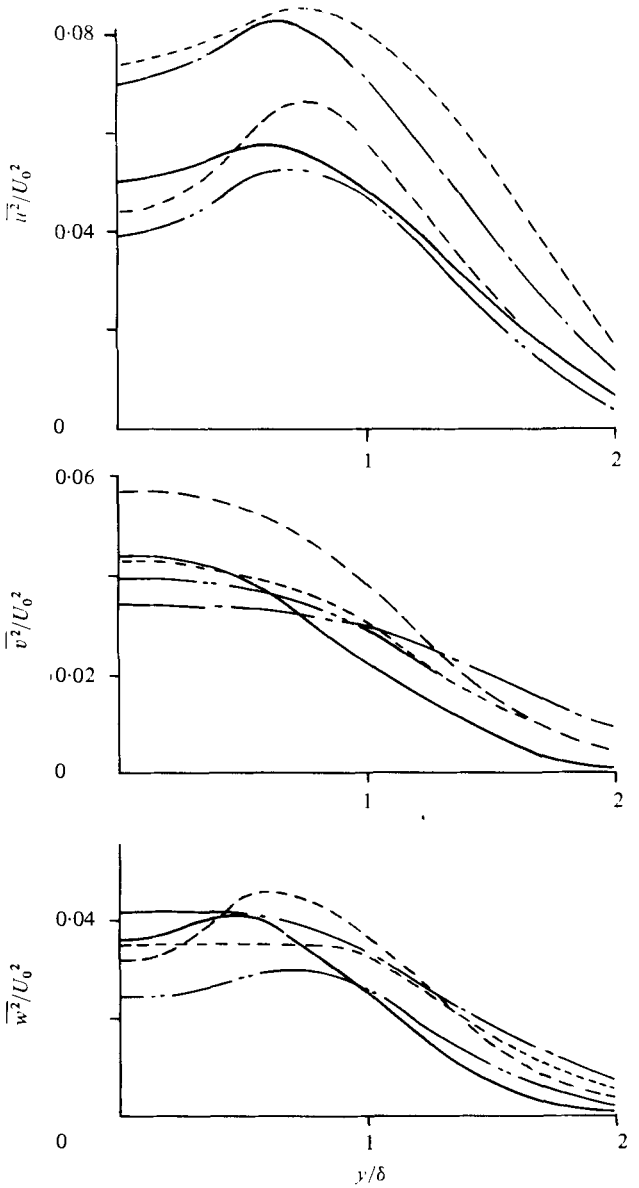

FIGURE 5. Turbulence normal-stress profiles for strong jets. Symbols as in figure 4.

'puffing' and 'flapping' at the jet nozzle may explain some of the differences shown but there is no direct evidence to support this.

The intermittency results for strong and weak jets, with the exception of Heskestad's, which are discussed by Gutmark & Wygnanski, agree quite well and give the point at which the intermittency factor γ_g is 0·5 as $y = 1{\cdot}78\delta$ with a standard deviation about this point of approximately $0{\cdot}45\delta$. The interface crossing rate n_i appears to be a maximum between $y = 1{\cdot}5\delta$ and $1{\cdot}7\delta$ and over this range γ varies from about 0·7 to 0·55 (figure 6). This implies that the bounding surface is not symmetric about the

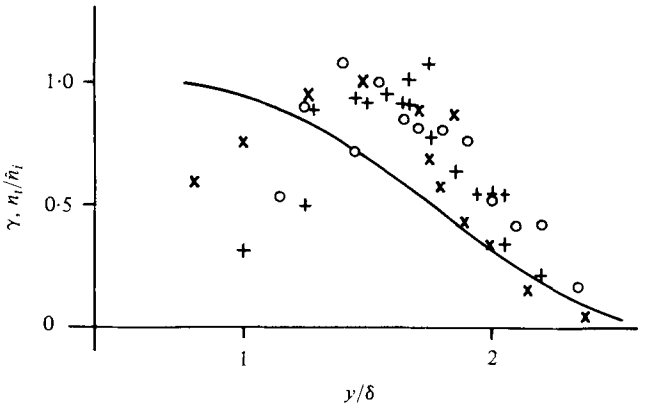

FIGURE 6. Intermittency (solid line) and normalized interface crossing rate. ○, Robins, $x/h = 100$; +, Bradbury, $x/h = 44, 71$; ×, Gutmark & Wygnanski, $x/h = 120$.

$\gamma = 0{\cdot}5$ point, but is more sharply folded in its troughs than on its crests. Direct observation of the mean durations of turbulent and non-turbulent flow support this description. The profiles of $n_i/\hat{n}_i$, where $\hat{n}_i$ is the maximum crossing rate, show some scatter, particularly towards the central region of the flow. As it becomes progressively more difficult to differentiate between zero-crossings owing to turbulence and interface motion as $\gamma \to 1$, this might reflect the technique used to evaluate n_i rather than any true scatter. The values of the maximum crossing rate quoted by Bradbury (1965) are

$$\hat{n}_i \delta / U_m = 0{\cdot}3 \pm 0{\cdot}1,$$

which agree with the present values of between 0·2 and 0·3, it being assumed that $U_m = U_1 + \frac{1}{2}U_0$. The flatness factors rapidly increase in the intermittent region and are constant (3·0) in the central region of the jet. The skewness factors of u and v steadily increase with distance from the jet centre, reaching a value of about 0·5 at $y = \delta$ (where $\gamma = 1$), which indicates that the probability distribution functions of u and v develop a positive-going tail.

Measurement of the diffusion and dissipation terms of the Reynolds-stress transport equations is difficult because of problems associated with hot-wire inaccuracies in the first case and problems associated hot-wire length effects and the choice of convection velocities in the second. For a jet in still air the direct application of Taylor's hypothesis is not justified, though it is possible to define a modified form of the hypothesis from the Navier–Stokes equations. Heskestad (1965*b*) applied order-of-magnitude arguments to the exact equation for $\overline{(\partial u_i/\partial t)(\partial u_j/\partial t)}$ and then time averaged the result and obtained equations for $\overline{(\partial u_i/\partial t)^2}$, $\overline{(\partial v/\partial t)^2}$ etc. Strictly speaking, the order-of-magnitude arguments should be applied to the time-averaged equations, though the end result is the same. An alternative approach is to use Taylor's hypothesis but with an effective velocity equal to the bulk convection velocity $U + u_i^2 u/q^2$. Both these approaches produce dissipation profiles for a jet in still air which are plausibly shaped and similar to those obtained for a jet in a moving stream by direct application of Taylor's hypothesis. Application of the convection-velocity hypothesis results in a distribution of dissipation very much like that obtained in a jet in a moving stream, whereas application of the modified Taylor hypothesis gives a distribution similar to

		Convection velocity		Modified Taylor hypothesis	
η	q^2/U_0^2†	$\epsilon\delta/U_0^3$	L_ϵ/δ	$\epsilon\delta/U_0^3$	L_ϵ/δ
0	0·130	0·0140	3·35	0·0105	4·46
0·5	0·145	0·0145	3·81	0·0110	5·02
1	0·115	0·0120	3·25	0·0112	3·48
1·5	0·055	0·0060	2·15	0·0090	1·43
2	0·015	0·0015	1·22	0·0045	0·41

† Mean of Robins' and Bradbury's data.

TABLE 3. Dissipation and dissipation length scales for developed jet.

	$\frac{y}{\delta}$	$\overline{\left(\frac{\partial v}{\partial t}\right)^2}\Big/\overline{\left(\frac{\partial u}{\partial t}\right)^2}$	$\overline{\left(\frac{\partial w}{\partial t}\right)^2}\Big/\overline{\left(\frac{\partial u}{\partial t}\right)^2}$
Jet in still air	0	1·5	1·5
	1·0	1·0	1·0
Strong jet	0	1·1	1·1
	1·0	1·0	1·0
Weak jet	0	1·7	1·3
	1·0	1·7	1·5

TABLE 4. Measured structure parameters for small-scale turbulence.

that presented by Gutmark & Wygnanski. As the data for a jet in a moving stream were obtained by the direct application of Taylor's hypothesis (the flow being more suited to the assumptions implicit in the hypothesis) it may be tentatively concluded that the convection-velocity hypothesis is slightly better than the modified Taylor hypothesis. This conclusion is reinforced by consideration of the dissipation length scale L_ϵ, defined by $\epsilon = q^3/L_\epsilon$, as this is expected not to be a rapidly varying function of η. Table 3 shows that the length scale calculated from the convection-velocity hypothesis is indeed more uniform than that calculated from the modified Taylor hypothesis data. No clear picture emerges as to the structure of the small-scale motion; indeed, Gutmark & Wygnanski's data indicate that the dissipation does not take a self-preserving form for $x < 120h$, which is in contradiction to Heskestad's results. The measurements summarized in table 4 suggest that the local isotropy conditions $\overline{(\partial v/\partial x)^2} = 2\overline{(\partial u/\partial x)^2}$, etc., do not hold. This being so, the difference between the two dissipation formulae

$$15\nu\overline{(\partial u/\partial x)^2}, \quad 3\nu\{\overline{(\partial u/\partial x)^2} + \overline{(\partial v/\partial x)^2} + \overline{(\partial w/\partial x)^2}\}$$

is considerable, i.e. 66 % at $y = \delta$. It is not surprising that the dissipation results usually have to be scaled in order for the integrated turbulent energy equation to balance.

All the triple velocity products ($\overline{u^2v}$, $\overline{v^3}$, $\overline{w^2v}$ and $\overline{uv^2}$) occurring in the transport equations for the turbulent energy and shear stress can be measured, though not very accurately. The results for jets in still air (figure 7) agree reasonably well but it must be emphasized that the gradients of these terms cannot be accurately evaluated. Hence care should be exercised in interpreting the local imbalances in the energy equations plotted by Bradbury (1965), Heskestad and Gutmark & Wygnanski as an

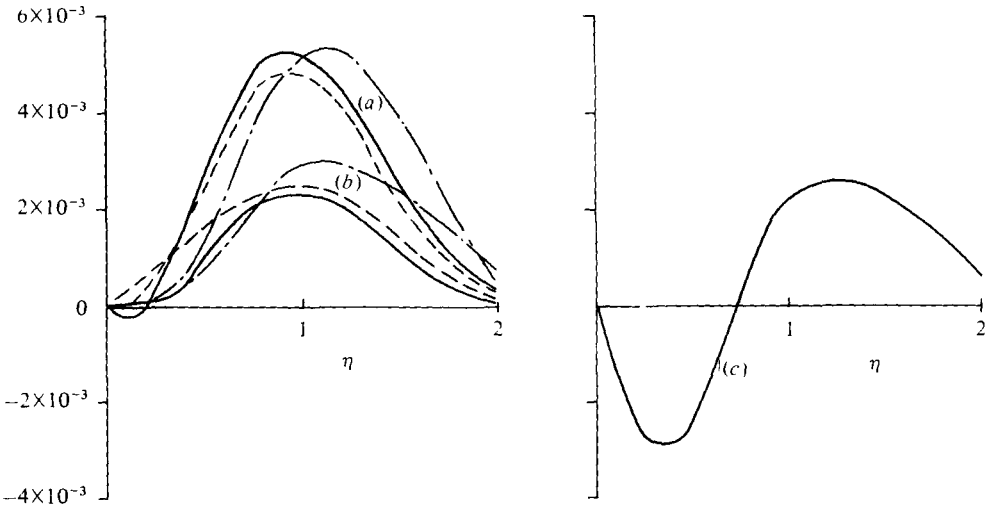

FIGURE 7. Triple products occurring in the shear-stress and energy transport equations. (*a*) $\overline{u_i^2 v}/U_0^3$. (*b*) $\overline{uv^2}/U_0^3$. (*c*) $(\overline{u_i^2 v} + \overline{2p^2 v/\rho})/U_0^3$. ——, Robins; – – –, Gutmark & Wygnanski; – – – –, Heskestad.

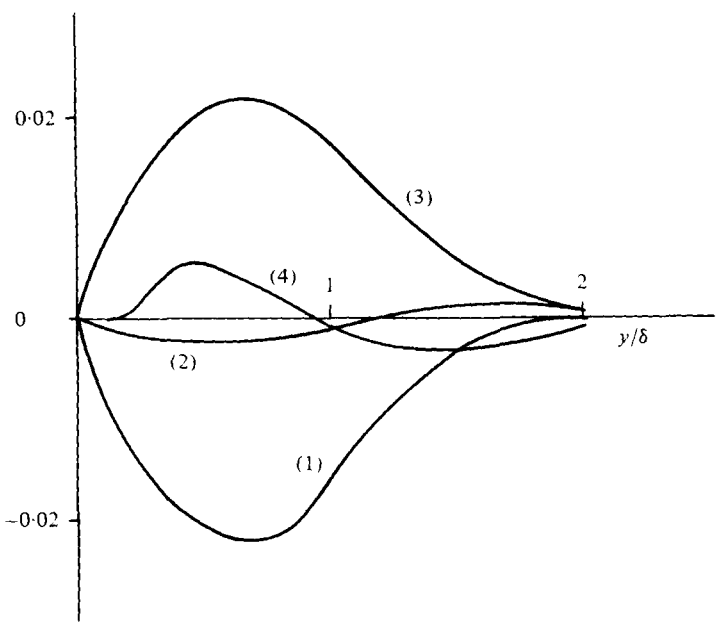

FIGURE 8. Distribution of terms in shear-stress transport equation for jet in still air. (1) Production, $(\delta/U_0^3)\,\overline{v^2}\,\partial U/\partial x$. (2) Advection, $(\delta/U_0^3)\,U_j\,\partial\overline{uv}/\partial x_j$. (3) Pressure–strain, $(\delta/U_0^3) \times \overline{p'/\rho(\partial u/\partial y + \partial v/\partial x)}$. (4) Diffusion, $(\delta/U_0^3)\,\partial\overline{uv^2}/\partial y)$.

indication of the pressure diffusion term $\partial(\overline{pv}/\rho)/\partial y$. However, the entire triple-product term of the energy equation, $\overline{u_i^2 v} + \overline{2p'v}/\rho$, can be approximately determined from the equation, and this too is plotted in figure 7. The complete term, unlike $\overline{u_i^2 v}$, correlates reasonably well with $-L_d q\,\partial(\frac{1}{2}q^2)/\partial y$, being negative near the jet centre and zero at about $\eta = \frac{3}{4}$, which is roughly the point of maximum turbulent energy.

Most of the terms in the shear-stress transport equation can be measured and if it is assumed that the pressure–transport term can be ignored then the pressure–strain term may be evaluated. Figure 8 shows the results thus obtained and demonstrates that the approximation production = pressure–strain is valid over the majority of the flow. Bradshaw (1969) has suggested that the pressure–strain term may be represented by

$$\overline{p(\partial u_i/\partial x_j + \partial u_j/\partial x_i)} \propto [uu]\,\partial U/\partial y + [uuu]/L,$$

where L is a length scale and the quantities in square brackets are combinations of Reynolds stresses. Consideration of the sign of the pressure–strain term on either side of the jet centre-line leads to the following expression:

$$\overline{p(\partial u_i/\partial x_j + \partial u_j/\partial x_i)} \propto q^2\,\partial U/\partial y + q\overline{uv}/L,$$

which when substituted into the production = pressure–strain form of the shear-stress transport equation gives, assuming $\overline{v^2} \propto \overline{q^2}$,

$$\overline{uv} \propto -qL\,\partial U/\partial y,$$

which is a variable-eddy-viscosity formula.

4.2. *Spectra and correlations*

Spectra of the non-zero Reynolds stresses were measured at a number of points in the central region of the jets. Typical results obtained in a jet in still air at $x = 100h$, $y = 0{\cdot}4\delta$ are shown in figure 9, where the power spectral densities were plotted in such a way that they would collapse in the inertial subrange if the expected Kolmogorov behaviour was exhibited. It can be seen that, although a very limited subrange appears to exist, the collapse is poor. This is somewhat surprising because the conditions for the existence of an inertial subrange are more than adequately satisfied; e.g. the turbulent Reynolds number is approximately 400 over the central region of the jet. However, in addition to the errors in the turbulence-intensity data, the local mean velocity may well not be the true convection velocity, which itself could be a function of frequency, and the data must be considered inconclusive. Similar subrange behaviour was observed in a jet in a moving airstream, though the spectral peaks at about $n\delta/U = 0{\cdot}1$ were not as prominent.

The correlation functions $R_{11}(r, 0, 0)$, $R_{11}(0, r, 0)$ and $R_{11}(0, 0, r)$ were measured at several positions within the jet flows; the results for separations in the x and z directions were similar to those presented by Gutmark & Wygnanski. Figure 10 shows measurements of $R_{11}(0, r, 0)$ in jets in still air, the correlation being defined as

$$R_{11}(0, r, 0) = \overline{u(\mathbf{x})\,u(\mathbf{x} + \Delta y)/u^2(\mathbf{x})},$$

where $\mathbf{x}$ is the position of the fixed probe. The most obvious feature of the results is the large negative lobe that occurs whenever the fixed and moving probes are on opposite sides of the jet centre-line. This feature, which was also observed by Gutmark & Wygnanski and Goldschmidt & Bradshaw (1973) (for the jet blowing apparatus used by Robins 1973), indicates a substantial degree of correlation between the large-scale motions on either side of the jet centre-line. However, strong negative lobes were

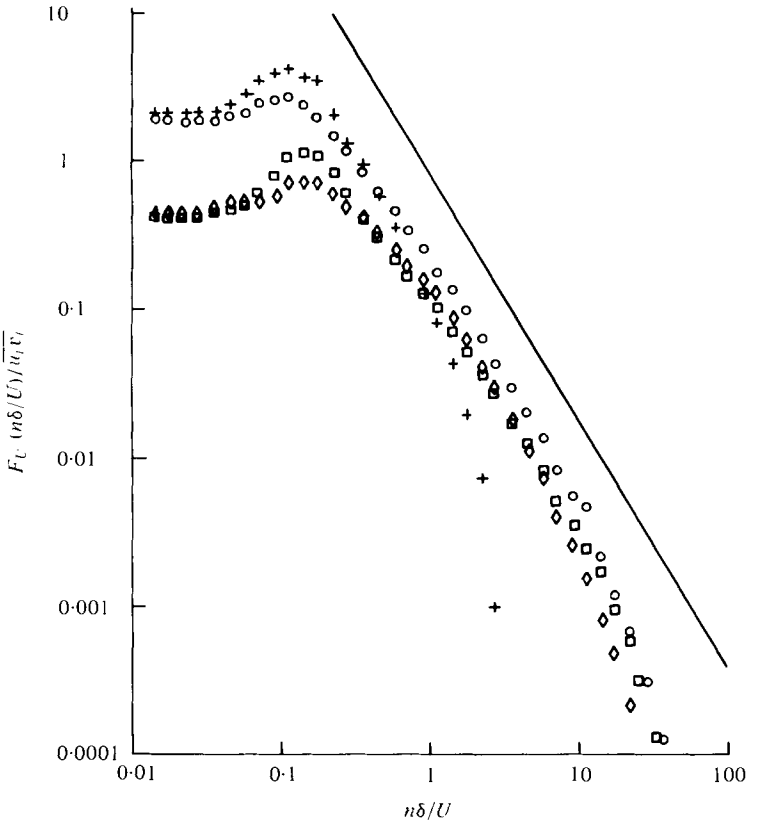

FIGURE 9. Spectral density functions at $y = 0{\cdot}4\delta$, $x = 100h$ for a jet in still air. ○, F_{11}; □, $F_{22}3v^2/4u^2$; ◇, $F_{33}3w^2/4u^2$; +, F_{12}.

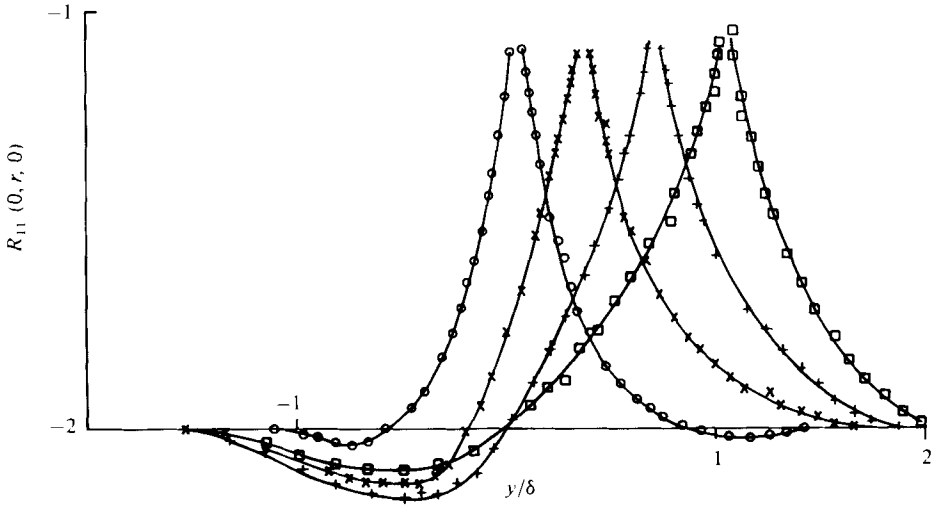

FIGURE 10. The correlation function $R_{11}(0, r, 0)$ for a jet in still air.

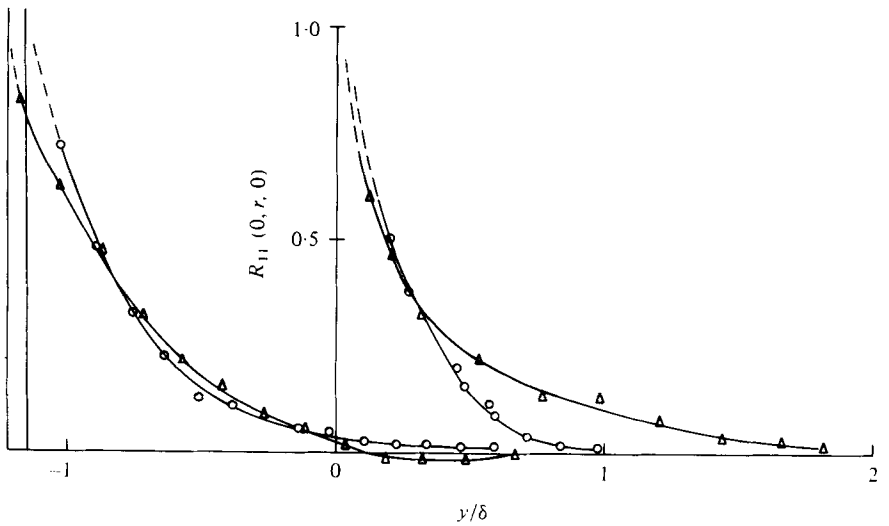

FIGURE 11. The correlation function $R_{11}(0, r, 0)$ for a jet in a moving stream. ○, strong jet; △, weak jet.

y/δ	0·05	0·37	0·71	1·04
$\int_0^\infty R_{11}(r, 0, 0)\, dr/\delta$†	0·35	0·45	0·48	0·55
$\int_0^\infty R_{11}(r, 0, 0)\, dr/\delta$‡	0·40	0·4	0·5	—
$\int_0^\infty R_{11}(0, r, 0)\, dr/\delta$	0·22	0·32	0·33	0·31
$\int_{-\infty}^0 R_{11}(0, r, 0)\, dr/\delta$	0·18	0·12	0·13	0·28
$\int_0^\infty R_{11}(0, 0, r)\, dr/\delta$	0·22	0·25	0·25	0·17

† $R_{11}r$ positive in the $-x$ direction.
‡ From power spectral density measurements.

TABLE 5. Integral scales for jet in still air.

not observed in a jet in a moving stream, as can be seen in figure 11, which shows the correlation

$$R_{11}(0, r, 0) = \overline{u(\mathbf{x})\, u(\mathbf{x}+\Delta y)}/\{\overline{u^2(\mathbf{x})\, u^2(\mathbf{x}+\Delta y)}\}^{\frac{1}{2}}.$$

Indeed, the results for both the strong and the weak jets are remarkably similar to those given by Grant (1958) for a two-dimensional turbulent wake.

Integral-scale values obtained from the spectra and correlation measurements in jets in still air are listed in table 5. The results are consistent with those of Gutmark & Wygnanski, but because of differences in the measurement technique quantitative agreement cannot be expected. It is worth noting that the standard deviation of the intermittency distribution about the point at which $\gamma = 0{\cdot}5$ is of the same order of

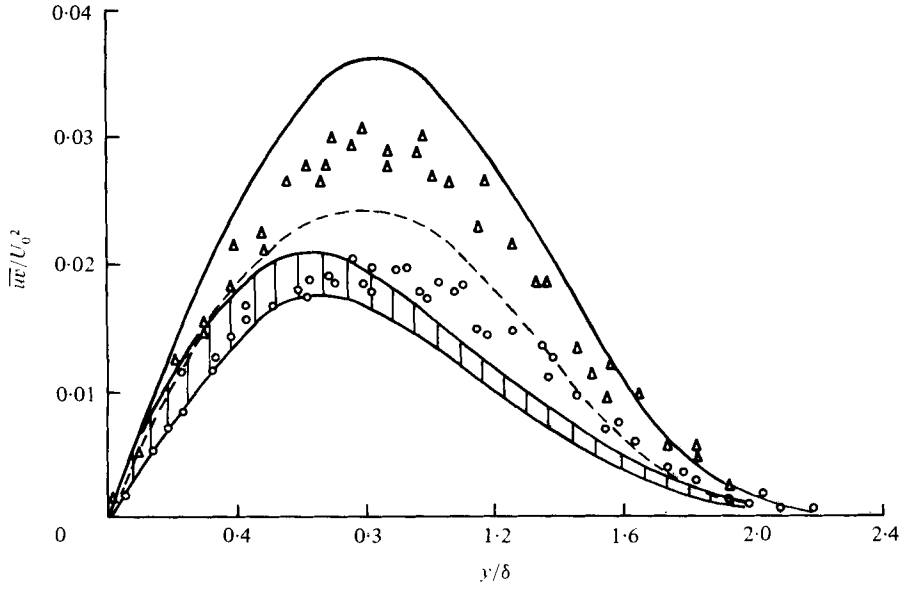

FIGURE 12. Measured shear-stress profiles for a jet in a moving stream. ○, strong jet; △, weak jet; Everitt; – – –, Bradbury; ||||, jet in still air, Robins; ——, wake, Everitt.

magnitude as the lateral integral scales. In general the scales increase slowly with increasing distance from the jet centre-line and begin to decrease only when the moving probe enters the jet edge.

5. Jet issuing into a parallel moving stream

It has already been noted that the present values for the non-dimensional longitudinal turbulence intensity $\overline{u^2}/U_0^2$ exhibit a slow increase with the velocity ratio U_1/U_0 and hence with downstream distance (figure 1). Although Gutmark & Wygnanski conclude that the data on the longitudinal turbulence intensity indicate that self-preservation (i.e. $\overline{u^2}/U_0^2$ = constant on $y = 0$) occurs at about $x = 40h$, the present results show that the addition of even a weak external stream is sufficient to prevent the normal stresses from attaining a self-preserving form. To study this in more detail the structure of the turbulence was investigated for two velocity ratios: one typical of a strong jet flow, with $U_0/U_1 \simeq 5$ (Bradbury's value was 6); the other typical of a weak jet flow, with $U_0/U_1 \simeq 0{\cdot}2$. Results from the strong jet are directly comparable with Bradbury's, while those for the weak jet make an interesting comparison with those from a nearly self-preserving, small deficit wake (Everitt 1972).

The measured shear-stress values in the strong jet (figure 12) are significantly lower than those given by Bradbury (1965); for $y/\delta < 1$ they are in good agreement with the present data for a jet in still air. However, the addition of an external stream and the consequent lower local turbulent intensities near the jet edge did not improve the agreement between the measured and calculated values. Normal-stress values for the strong jet (figure 13) show considerable variations from those obtained in other jet flow experiments, a feature implied by the data presented in table 2. The

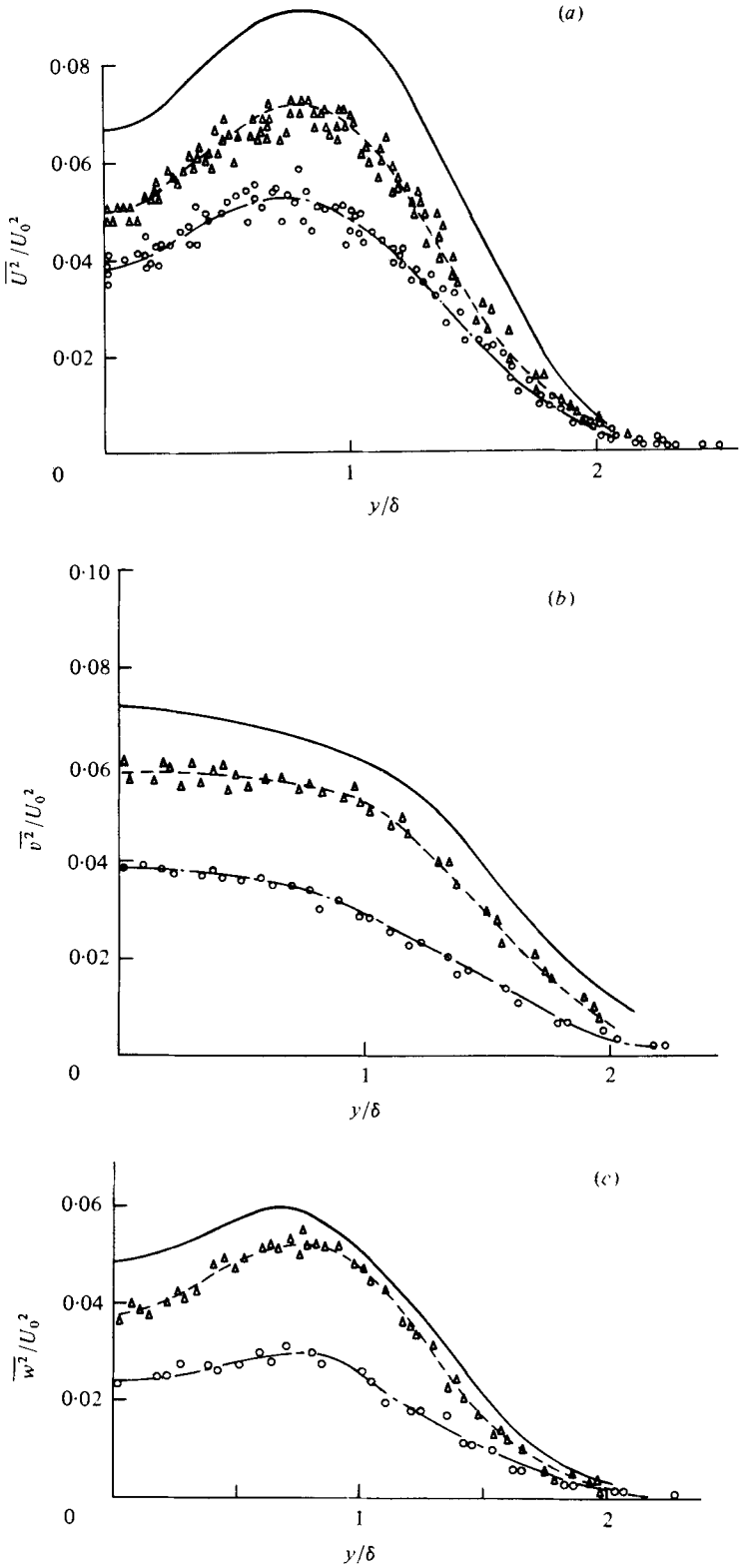

FIGURE 13. Normal-stress profiles for a jet in a moving stream.
—— –, strong jet; – – –, weak jet; ——, wake.

y/δ		0	1·0/1·1
Strong jet	$\int_0^\infty R_{11}(r, 0, 0)\, dr/\delta$	0·53	—
	$\int_0^\infty R_{11}(r, 0, 0)\, dr/\delta$†	—	0·48
	$\int_0^\infty R_{11}(0, r, 0)\, dr/\delta$	0·30	0·40
Weak jet	$\int_0^\infty R_{11}(r, 0, 0)\, dr/\delta$	0·71	—
	$\int_0^\infty R_{11}(r, 0, 0)\, dr/\delta$†	—	0·61
	$\int_0^\infty R_{11}(0, r, 0)\, dr/\delta$	0·45	0·52
Wake	$\int_0^\infty R_{11}(r, 0, 0)\, dr/\delta$	—	1·15

† From power spectral density measurements.

TABLE 6. Integral scales for jet in moving stream.

$\overline{u^2}$ profile is slightly lower than Bradbury's and much lower than that for a jet in still air. In the central region of the jet the present $\overline{v^2}$ profile for the strong jet is again in better agreement with data for a jet in still air than with Bradbury's, while the $\overline{w^2}$ profile, though showing a saddle shape similar to Bradbury's, is considerably smaller in magnitude. In the case of the weak jet the normal- and shear-stress profiles exhibit a considerable increase over the equivalent values for the strong jet, while remaining well below the corresponding wake values. Gutmark & Wygnanski suggested that the addition of a weak external stream may have a profound effect on the state of self-preservation. In support of this they remarked that the high ratio of the maximum longitudinal intensity to the centre-line value implied by Bradbury's results was indicative of a lack of true self-preservation. The present results show similar high values, 1·4 for both the strong and the weak jets, while the value for the wake, which was much closer to self-preservation than the jet, is similarly high at 1·3. Clearly, the turbulent structure of a jet in a parallel stream is constantly changing and, like that of a wake (Townsend 1976, p. 225), shows a similar slow approach to self-preservation.

The $R_{11}(0, r, 0)$ data shown in figure 11 indicate an increase in the integral scale in passing from the strong to the weak jet, though the overall shapes are similar and the negative lobes evident in figure 10 are absent. The integral-scale values listed in table 6 define the increase in the relative size of large eddies, though it should be noted that this increase in no way accounts for the difference between jet and wake values.

6. Discussion

Both a jet in still air and a jet in a parallel moving stream quickly develop a similar mean-velocity profile, though the addition of an external stream constrains the latter jet to a slower, nonlinear spread.

Although hot-wire measurements in a two-dimensional jet without an external

stream are unlikely to be very accurate, especially in the outer regions of the flow, this cannot readily explain all of the scatter shown by the various investigations. Indeed, there is considerable variation between the present results and those of Bradbury (1965) for a jet in an external stream even though the local turbulence intensities and flow directions are unlikely to be as detrimental to hot-wire accuracy as in a free jet. Both Gutmark & Wygnanski and Goldschmidt & Bradshaw have tentatively suggested that initial conditions may be important. Whereas this is almost certainly true in the development region, it is difficult to explain a continued influence in a region of true self-preservation unless jet 'flapping' and 'puffing' are important. It is interesting to note that the different investigations of a jet in still air give similar $\overline{v^2}/U_0^2$ profiles, which suggests that any flapping is not related to nozzle conditions but is either a feature of the turbulence itself or some basic flow instability, though reasons for the high longitudinal intensities observed by Heskestad and Gutmark & Wygnanski cannot be stated. Obviously there is a need for further work on this question, possibly using laser or pulsed-wire anemometry to overcome the problems inherent in using hot-wire anemometers in flows of high turbulence intensity.

The normal-stress and shear-stress profiles do, however, exhibit an important difference between jets with and without an external stream. Clearly the addition of an external stream removes the possibility of true self-preservation of the turbulent structure. The turbulent intensities $\overline{u^2}/U_0^2$ etc. and the shear stress $\overline{uv}/U_0^2$ increase slowly with distance from the nozzle although they remain well below the comparable values for a two-dimensional wake. It should, perhaps, be noted that in both of the present strong jet flows there was a marked difference between the measured and calculated shear-stress profiles.

Measurement difficulties imply that definite conclusions concerning the state of the small-scale structure cannot be reached. For the measurements made in the jet in still air the turbulence Reynolds number $(\overline{u^2})^{\frac{1}{2}}\lambda/U$, where λ is defined by the relation $\epsilon = 15\nu\,\overline{u^2}/\lambda^2$, fell from about 300 at $y = 0$ to about 200 at $y = \delta$ and the dissipation length scale L_ϵ was in excess of a thousand times the Kolmogorov length scale $(\nu^3/\epsilon)^{\frac{1}{4}}$. These values are sufficiently large to indicate the existence of both a significant inertial subrange in the velocity spectra and local isotropy of the small-scale motion. However, spectra and dissipation measurements do not support these conclusions and the matter must be left for clarification by further experiments in jet flows at a very high Reynolds number. Although the problem of defining suitable convection velocities remains, they could be measured by methods similar to those employed by Wygnanski & Fiedler (1969).

Approximately 80% of the shear stress and 40% of the turbulent energy in a jet in still air resides in an identifiable large-scale motion which also seems to be responsible for the large-scale features of the turbulent interface. The large-scale motions on either side of the jet are strongly negatively correlated, a feature which has been observed by several investigators and is suggestive of a large-scale motion which can best be described as 'local flapping'. However, the present results for a jet in a moving stream contradict this observation, and Grant (1958) found no such correlations in a two-dimensional wake. Further investigations of all the two-point correlation functions in jets with and without external streams are required before the nature of the large-scale motions can be ascertained, though it appears that the addition of even a weak external stream may be sufficient to inhibit local flapping.

The shear-stress transport equation for a jet in still air reduces to the variable-eddy-viscosity formula

$$\overline{uv} = -Lq\partial U/\partial y.$$

Furthermore, as the dissipation of turbulent energy is roughly correlated with q^3/L_ϵ and the lateral diffusion of turbulent energy with $-\partial/\partial y(L_d q\,\partial(\frac{1}{2}q^2)/\partial y)$ it is possible to use the turbulent energy equation together with the momentum equation to calculate the flow properties. This possibility was tested by making use of the formal self-preserving character of the equations and then numerically integrating the resulting set of equations for the dependent variables $\overline{uv}$, q and U in terms of the single independent variable y/δ; the procedure is described in the appendix. By suitable choice of the three length scales L, L_ϵ and L_d, good agreement was obtained between predicted and measured properties of strong jets. In order to use the equations to calculate two-dimensional self-preserving wake flows it was found necessary to increase L by about 60 % and to reduce L_ϵ and L_d slightly. It therefore follows that the main problem to be overcome in predicting the development of a jet in a moving stream lies in adequately describing the behaviour of the length scale L.

The authors would like to thank Dr L. J. S. Bradbury and the staff of the Aeronautics Department at Imperial College for their help and encouragement during the course of this research. Thanks are also due to the Science Research Council for the provision of grants.

Appendix

The equations to be solved are those of continuity, momentum, turbulent energy and shear stress. With the use of the approximations discussed in §6 the last two can be written as

$$\tfrac{1}{2}(U\partial/\partial x + V\partial/\partial y)q^2 + \overline{uv}\,\partial U/\partial y - \partial/\partial y(L_d q\,\partial(\tfrac{1}{2}q^2)/\partial y) + q^3/L_\epsilon = 0,$$

$$\overline{uv} = -Lq\partial U/\partial y.$$

For a strong jet the equations can be shown to permit a self-preserving solution for which $\delta = ax$ and $U_0/U_j = b(x/h)^{-\frac{1}{2}}$, and by writing

$$U/U_0 = f(\eta), \quad q^2/U_0^2 = g_0^2 g^2(\eta), \quad uv/U_0^2 = g_{12}(\eta),$$

where $\eta = y/\delta$, the equations of motion become

$$f' = -C_1 f \int_0^\eta f\,dt/g,$$

$$g'' = \left\{C_4 g^2 - C_2\left(g\int_0^\eta f\,dt\right)' - C_3 f'^2 - 2g'^2\right\}\Big/ g,$$

$$g_{12} = -(a/C_1)gf',$$

where $C_1 = a\delta/2g_0 L$, $C_2 = a\delta/2g_0 L_d$, $C_3 = L/L_d g_0^2$, $C_4 = \delta^2/L_\epsilon L_d$.

The boundary conditions for f and g are

$$f'(0) = g'(0) = 0, \quad f(0) = g(0) = 1,$$

$$f(\pm\infty) = f'(\pm\infty) = \ldots = 0, \quad g(\pm\infty) = g'(\pm\infty) = \ldots = 0,$$

$$f, g \geqslant 0.$$

It can be shown that the equations and boundary conditions are invariant under the following transformations:

$$f \equiv f, \quad g \equiv g, \quad \eta \equiv \alpha\eta, \quad g_{12}/a \equiv \alpha g_{12}/a,$$
$$C_1 \equiv C_1/\alpha^2, \quad C_2 \equiv C_2/\alpha^2, \quad C_3 \equiv C_3, \quad C_4 \equiv C_4/\alpha^2.$$

Hence a solution to the equations may be found by holding C_1 fixed and adjusting C_2, C_3 and C_4 until predictions satisfying the boundary conditions at infinity have been found. When such a solution has been found it can be converted to a convenient form by choosing α such that $f(\eta = 1) = \frac{1}{2}$.

The solution procedure was based on a Milne predictor–corrector method for which the error term is $O(H^5)$, where H is the step length. Calculations for the first two steps, together with the symmetry conditions, provided enough values to start the predictor–corrector, and the boundary conditions at the jet edge were effectively replaced by

$$|f|, |f'|, |g|, |g_{12}| = O(\sigma), \quad \sigma \ll 1.$$

A step length of $H = 0{\cdot}005$ was used and once a solution had been obtained the results were recalculated for $H = 0{\cdot}01$, a process which tended to introduce differences into the fourth significant figure. Because the boundary conditions at infinity were only approximately satisfied acceptable solutions could be obtained for a variety of values of the parameters $C_1, \ldots, C_4$. The solutions to be discussed were chosen on the basis of reasonable values for the centre-line turbulent energy g_0^2. Because use has been made of the self-preservation condition, the rate-of-spread constant a cannot be calculated, though conservation of momentum gives the velocity-decay constant b as

$$b^2 = C_M \Big/ a \int_{-\infty}^{\infty} f^2 d\eta,$$

where C_M is the momentum flux coefficient.

A similar procedure was adopted for the asymptotic calculations of weak jets or wakes, the self-preserving conditions being

$$U = U_1 \pm U_0 f(\eta), \quad \delta/d = a(x/d)^{\frac{1}{2}}, \quad U_0/U_1 = b(x/d)^{-\frac{1}{2}}$$

and the equations of motion

$$f' = -C_1 f/g,$$
$$g'' = \{C_4 g^2 - C_2(\eta g)' - C_3 f'^2 - 2g'^2\}/g,$$
$$g_{12} = \mp (m/C_1) g f',$$

where $m = /a2b$ and

$$C_1 = m\delta/g_0 L, \quad C_2 = m\delta/g_0 L_d, \quad C_3 = L/L_d g_0^2, \quad C_4 = \delta^2/L_e L_d.$$

Conservation of momentum gives

$$b = C_M \Big/ a \int_{-\infty}^{\infty} f d\eta,$$

where C_M is the momentum excess, or deficit, flux coefficient.

Mean-velocity profiles were well predicted for both flows, though this is scarcely surprising, especially as a constant-eddy-viscosity solution adequately predicts the

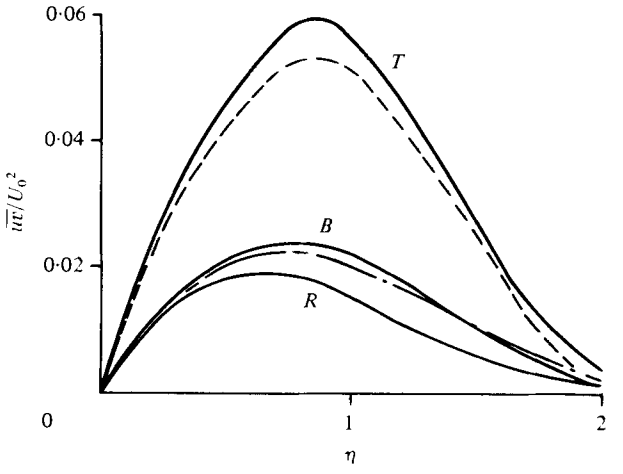

FIGURE 14. Predicted and measured shear-stress profiles. Measurements: *R*, jet, Robins; *B*, jet, Bradbury; *T*, wake, Townsend. Predictions: ———, jet; – – –, wake.

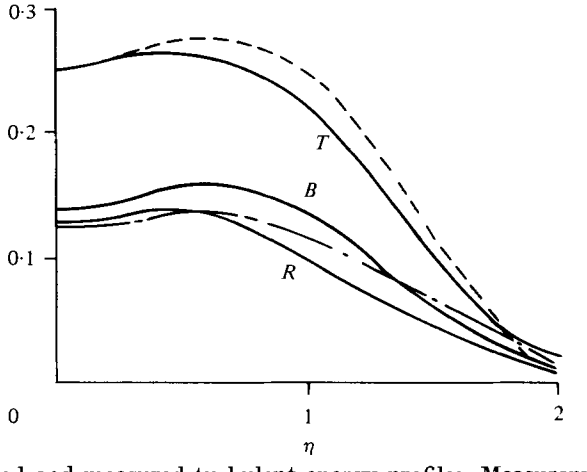

FIGURE 15. Predicted and measured turbulent energy profiles. Measurements: *R*, jet, Robins; *B*, jet, Bradbury; *T*, wake, Townsend. Predictions: ———, jet; – – –, wake.

	Strong jet flow		Wake flow	
	Predicted	Measured	Predicted	Measured
L/δ	0·089	0·10†	0·139	0·14§
L_ϵ/δ	3·90	3·4†, 3·7	3·33	3·2§
L_d/δ	0·178	0·1†	0·139	—

† Robins (1973).
‡ Bradbury (1965).
§ Townsend (1976).

TABLE 7. Predicted and measured length scales.

profiles over much of the flows. Figures 14 and 15 show comparisons of measured and predicted shear-stress and energy profiles, and table 7 gives the values of L, L_d and L_ϵ calculated from the parameters $C_1, \ldots, C_4$. In calculating the shear stress and length scales the parameters a and m have been taken as 0·1. It can be seen that the agreement between the measurements and predictions is quite good; no doubt it could be improved by further refining the values of $C_1, \ldots, C_4$, though this did not seem worth pursuing. A two-dimensional calculation of the flow fields would, of course, yield values of a and m; the value of using the self-preserving form of the equations is that it provides a relatively simple means of testing turbulent modelling hypotheses. Of course, the procedure would become more complex if further equations were introduced, say to calculate the dissipation, as this would increase the number of parameters. However, in view of the success of the calculations this would not seem to be necessary, though it seems essential to include an equation for the length scale L, as this is approximately 60 % higher in a wake than in a jet. The differences in the values of L_ϵ and L_d are probably not too important, though it might be worthwhile replacing the constant-L_ϵ formulation by a universal distribution $L_\epsilon(y/\delta)$.

REFERENCES

Bradbury, L. J. S. 1965 *J. Fluid Mech.* **23**, 31.

Bradbury, L. J. S. 1967 *Aero. Quart.* **18**, 133.

Bradbury, L. J. S. & Riley, J. 1967 *J. Fluid Mech.* **27**, 381.

Bradshaw, P. 1969 *Boeing Sci. Res. Lab. Symp. Turbulence*, 1967.

Bradshaw, P. 1977 *J. Fluid Mech.* **80**, 795.

Champagne, F. H., Sleicher, C. A. & Wehrmann, O. H. 1967 *J. Fluid Mech.* **28**, 153.

Everitt, K. W. 1972 Ph.D. thesis, London University.

Goldschmidt, V. W. & Bradshaw, P. 1973 *Phys. Fluids* **16**, 3.

Grant, H. L. 1958 *J. Fluid Mech.* **4**, 149.

Guitton, D. E. 1968 *McGill Univ., Mech. Engng Dept. Rep.* no. 68–6.

Gutmark, E. & Wygnanski, I. 1976 *J. Fluid Mech.* **73**, 465.

Heskestad, G. 1965*a* *J. Appl. Mech.* **32**, 721.

Heskestad, G. 1965*b* *J. Appl. Mech.* **32**, 735.

Kotsovinos, N. E. 1976 *J. Fluid Mech.* **77**, 305.

Robins, A. G. 1973 Ph.D. thesis, London University.

Townsend, A. A. 1976 *The Structure of Turbulent Shear Flow*, 2nd edn. Cambridge University Press.

Wygnanski, I. & Fiedler, H. 1969 *J. Fluid Mech.* **38**, 577.